Development of a wave energy converter (WEC) design tool – application to the WaveRoller WEC including validation of numerical estimates

J. Lucas[1], M. Livingstone[1], M. Vuorinen[2] and J. Cruz[1]

[1]GL Garrad Hassan
St Vincent's Works, Silverthorne Lane, Bristol. BS2 0QD. UK
E-mail: Jorge.Lucas@gl-garradhassan.com

[2]AW-Energy Oy
Vanha Nurmijärventie 85, 01730 Vantaa, Finland
E-mail: Matti.Vuorinen@aw-energy.com

Abstract

The paper describes a new, fully coupled, wave energy converter (WEC) design tool, WaveDyn and its application to the design of the WaveRoller WEC. GL Garrad Hassan (GH) has been supporting AW-Energy (AWE) on the development of their commercial scale 'WaveRoller' machine, deriving independent numerical and experimental performance related predictions, namely load and absorbed power estimates.

WaveDyn allows users to load hydrodynamic data for a specific geometry, define a multi-body structural model with all associated physical links and characterize the power take-off (PTO) in detail, potentially incorporating internal PTO dynamics. The software also incorporates a moorings module whereby as user may apply nonlinear force profiles to specific points in the structure.

Under this work, all core WaveDyn modules have been used to iterate on a range of geometries, hydrodynamic theories, PTO target profiles (including nonlinearities) and technical constraints (e.g. maximum allowable PTO torque). The fully-coupled modelling approach allows the influence of major design variables on the complete system to be assessed. Some key results are presented here and compared with experiments conducted at 1:24 scale.

Keywords: Wave Energy, WaveDyn, Validation, WaveRoller, WECs

1. Introduction

AW-Energy is developing a technology named WaveRoller for harvesting wave energy from near-shore locations. WaveRoller is composed of hinged plates or 'flaps', anchored to the sea bed. The flaps are driven back and forth by the surge forces induced by the shallow water waves. The resulting kinetic energy is collected by a hydraulic power take-off (PTO); a hydraulic ram connected to the flap driving a motor/generator system. A demonstration unit rated at 300 kW is now ready to be deployed off the Portuguese coast at Peniche. AW-Energy has been working on the design of commercial-scale units which will be rated in the MW class.

The present paper describes the scale model tank tests of these commercial-scale units and the procedures performed to validate the numerical code being developed by GH to support AW-Energy research and development activities.

2. AWE WaveRoller scale model

The experimental tests performed by AWE follow a Froude scaling law to guarantee the dynamic similarity between the dominant forces (inertial and gravitational). A scale of 1:24 was selected and the experimental model was designed to reflect the main properties of the full scale prototype. In particular, the PTO was designed to keep at scale the same torque-velocity profile as the nominal full-scale machine.

A photograph of the WaveRoller scale model is shown in Figure 3.1. Experimental test have been performed with both single machines and arrays of three devices with identical geometry and mass properties. The flaps are positively buoyant and are

mounted on a seabed pontoon so that in calm water they sit vertically with a 0deg pitch angle. The majority of the PTO is located in the pontoon below the flap and, in the experimental models, this extends below the level of the tank floor. A deep, central pit in the wave basin facilitated this arrangement. The model flaps are hinged at their base, the hinges themselves being connected to an angular gearbox that redirects the rotational axis through 90° to drive a servo motor. A torque transducer is mounted on the servo motor axel. Control of the model is achieved by using a programmable machine drive unit supplied by ABB. The drive unit allows a demanded torque to be specified at the servo motor, in order to resist the motion of the flap.

Figure 1: WaveRoller scale model

A position sensor, internal to the servo-motor, was calibrated by moving the flap to known angular displacements and recording the output voltage. The torque transducer comes with a factory calibration certificate. The torque applied by the servo motor is controlled by the servomotor and drive unit internal components, the external transducer being used for measurement, but not control. The applied PTO torque profile was calibrated both on the test bench and in the water. On the bench, the PTO profile was calibrated by moving the flap manually at a range of representative wave frequencies and recording the signals from the torque transducer and angular sensor; The second calibration of the PTO profile was performed with the model in the tank to adjust some of the control parameters (filter lengths for the angle signal) with the model in the water, as the bench tests did not exactly recreate the flap motion under wave excitation .

The PTO drive unit was used for the data acquisition as well as to drive and control the model. The system has 8 available input channels. Each model requires two channels to record the torque and flap position. For the tests with three flaps this leaves 2 channels spare for recording other signals.

3. WaveDyn

WaveDyn is a multi-body, time-domain software simulation tool that has been developed by GH specifically for evaluating WEC performance. The software allows a user to construct a numerical representation of a WEC by connecting structural, hydrodynamic, PTO and moorings components in a fully-coupled manner through a flexible user interface.

The dynamics of the WEC are solved in the time domain using a fixed, or adaptive, variable timestep integrator implementation. At present the hydrodynamics module uses a quasi-linear formulation based on data calculated by a boundary element method (BEM) potential flow solver. Diffraction, radiation and non-linear hydrostatic effects and interactions are included in the model, however viscous effects are assumed negligible, with the machine response being largely dominated by reactive, rather than resistive, hydrodynamic forces.

Control actions may be implemented through the PTO components. WaveDyn allows dynamic or explicit PTO models to be applied to any joint in the system, where energy converted from the relative motion between adjacent bodies may be used to drive the WEC power-train.

WaveDyn structural models are built up incrementally, starting from a ‘Ground’ type structural component, which is used to locate the structure in the WaveDyn global reference frame. Each element in the model has what is referred to as a ‘proximal node’, which is the reference position for its own body-fixed reference plane. If a body has other bodies connected to it then it also has a ‘distal node’ which represents the connection point for the remainder of the structure. The distal node will also be the proximal node of the subsequent body. Joint elements, where the distal node may translate or rotate relative to the proximal one are a key feature of the implementation, allowing any number of freedoms to be represented. The nodes themselves are not part of the bodies, but describe how the structure is joined together. The spatial location of the elements in the model is specified through the inclusion of ‘rigid links’ which provide spatial displacements and fixed rotations relative to the previous node. A finite element assembly process is used by the engineering code to combine the individual component Lagrangian formulations in to a complete structural system.

Figure 2 shows the WaveDyn block diagram illustrating the components used to model the array of

WaveRoller devices. Each WEC is represented by a rigid body component connected to a pitching hinge. The measured mass and moments of inertia of the flap are introduced as the properties of the rigid body in addition to the hydrodynamic radiation and diffraction forces. The hydrodynamic forces are computed externally through a commercial flow solver. At present GH has implemented a plugin to process and upload automatically the hydrodynamic properties computed by WAMIT [1]. In the near future, this automatic importing capability will be extended to other commercial and GL Group flow solvers.

Note that the external flow solver provides the solution of the hydrodynamic problem in the frequency domain which is suited to describe a system in steady state. However, when a body is forced to move more generally, waves of all frequencies will be generated on the free surface. As time increases these waves propagate outward from the body but continuously affecting the fluid pressure and hence the body force for all subsequent times, introducing a 'memory effect' to the system (equivalent to a large number of unknown dynamic states). Therefore the radiation force needs to be described in a more general form which accounts for this phenomenon. A suitable description is given by Cummins [2]. Note also that such representation of the problem allows the introduction of more sophisticated models of the PTO with non-linear properties.

The WaveRoller PTO properties are introduced at the hinge element of the WaveDyn model. The PTO module of WaveDyn was designed to incorporate a number of different mathematical models. The joint kinematics (position, velocity and acceleration) are passed to the PTO module which calculates a resistive force to be applied at the joint and completes any internal calculations required to give an estimate of the electrical power output extracted. At the present stage of development, the PTO module allows the definition of simple models which are linear or polynomial functions of the velocity. More complex models have also been implemented to incorporate internal system dynamics and more complex loss models.

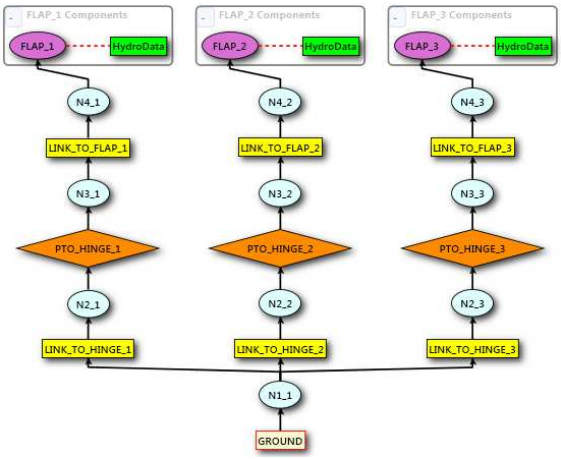

Figure 2: Block diagram representing the WaveDyn model of the three machine WaveRoller array.

The PTO model used for the simulations discussed here is based on a lookup table defining PTO force as a pricewise continuous function of the velocity and displacement in the joint. This implementation is very flexible as it allows the representation of generic non-linear functions.

4. AWE experimental tests

The experimental tests with the WaveRoller scale models were performed at the CEDEX (Centro de Estudios y Experimentación de Obras Públicas) multidirectional wave basin in Madrid, Spain.

The wave basin has dimensions of 34m x 32m (LxW). The maximum depth used for the experimental tests was 1.15m. On one of the basin's sides, is fitted with 72 independent piston wave makers. At its centre, there is a pit which is 3x3 m wide and which provides an additional depth of 1m.

This pit was used to house the PTO units of the WaveRoller scale models. On the opposite side to the wave paddles, the wave basin was fitted with a gravel beach, and both side walls were fitted with wire mesh structures containing perforated sheets for additional wave absorption. Active wave absorption control by the wave makers was not available. An overview of the basin is shown in Figure 3.

Figure 3: CEDEX multidirectional wave basin

One of the main objectives of the AWE experimental tests (and central to this paper) was to provide a dataset to be used to validate the numerical models and the performance estimates computed for the WaveRoller WEC operating in isolation and in an array. Other objectives of the tests were related with the investigation of the influence of a number of design variables on model performance.

The wave conditions selected for the experiments were measured in absence of the models, using a total of 14 wave probes. The location of the wave probes is shown schematically in Figure 4. Wave probe number 9 was centred on the location of the flap used in the single model experiments. Wave probes 8 and 10 were centred on top of the other two flaps used for the array experiments: for the array discussed here, the WaveRollers were placed in a line parallel to the wave makers. Wave gauge number 1 was used as a reference signal to synchronise the signals acquired by the AWE

(machine data) and CEDEX (wave probe data) data acquisition systems (DAQs).

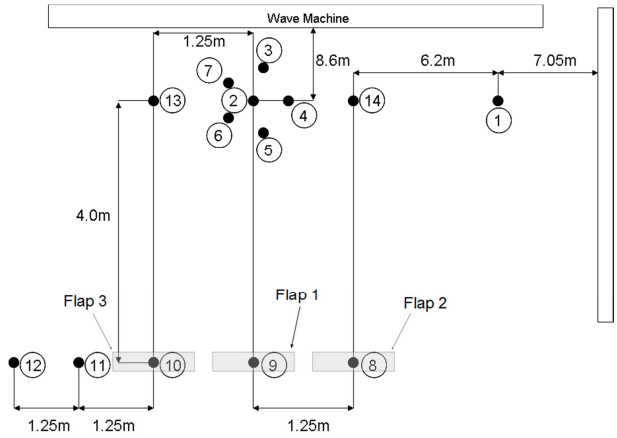

Figure 4: Schematics of the array of WaveRollers and location of the wave probes

The 6 wave probes numbered from 2 to 7 were located at the centre and corners of a pentagon and were used for the computation of directional spectra.

During the measurement of the calibration waves, the reflection coefficient of the wave basin was measured. It was found to be larger for the longer waves and to be in the range of 10% to 30%. (see Figure 5).

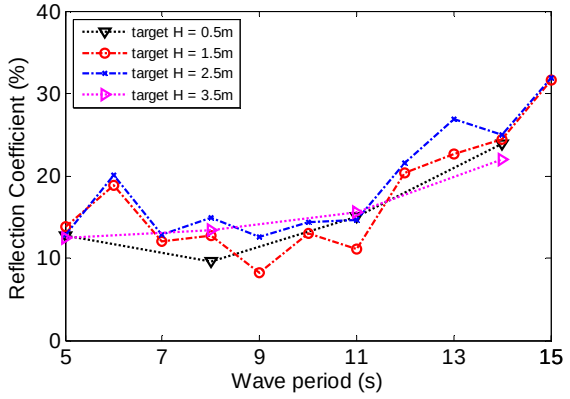

Figure 5: Measured reflection coefficient for regular waves, plotted against full-scale equivalent wave period

Large reflections were noticed during the tests and these has an impact on the quality of the wave field, especially during regular waves, for which 2nd and 3rd order harmonics and interference patterns were observed. Table 2 show the full scale equivalent energy period and significant wave height measured for the irregular, unidirectional waves. The mean values were computed over all wave probes. The differences to the target values are less than 10% for the wave height and 5% for the energy period. The columns associated with wave probe 9 show two independent measurements for the calibration waves. The differences found between the measurements are less than 5% for the significant wave height and less than 2% for the energy period. Figure 6 shows the measured spectra for two independent waves with full-scale H_{m0} = 1.5m and Te = 10 s. In the plot, the continuous black line shows the target spectrum. The main differences are found at the peak, where the measured value is about 40% below the target value. The analysis of the time series for this set of waves showed good repeatability in the input waves. An example of the time series is shown in Figure 7.

Table 1: Measured parameters for the calibration waves (irregular unidirectional, full-scale equivalent values)

Target		Wave Gauge 9		Average over all probes			
H_{m0} (m)	T_e (s)	H_{m0} (m)	T_e (s)	H_{m0} (m)		T_e (s)	
				mean	std	mean	std
1	8	0.901	8.096	0.946	0.1488	8.05	0.0869
		0.935	8.02				
1.5	6	1.42	6.178	1.450	0.0729	6.11	0.1116
		1.465	6.171				
1.5	10	1.308	9.992	1.369	0.1782	10.00	0.1539
		1.297	9.985				
2	8	1.842	8.331	1.871	0.0937	8.23	0.1563
		1.849	8.218				
2	12	1.695	11.913	1.821	0.1986	11.91	0.1775
		1.706	11.879				
2.5	10	2.271	10.334	2.359	0.1366	10.27	0.2500
		2.305	10.235				
2.5	14	2.245	13.632	2.300	0.3115	13.44	0.1548
		2.268	13.618				
3	12	2.681	11.994	2.801	0.2867	11.91	0.2362
		2.666	11.975				

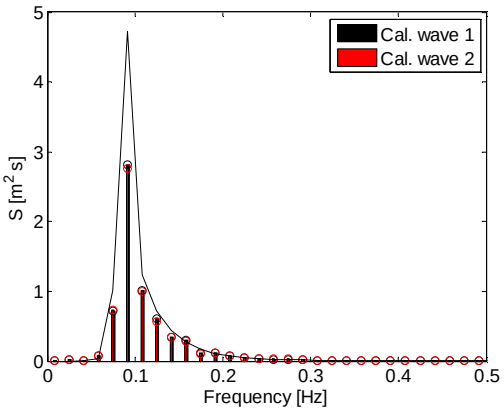

Figure 6: Comparison of measured spectra for two independent waves with H_{m0}=1.5 m and Te=10 s

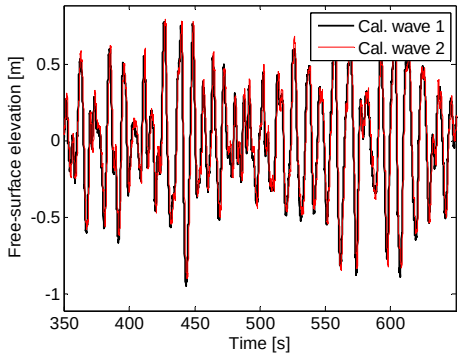

Figure 7: Comparison of measured time series for two repeat tests with H_{m0}=1.5 m and Te=10 s

5. Validation of the numerical estimates

WaveDyn models were built to reproduce the AWE experiments at CEDEX. The block diagram for the WaveDyn model structure associated with the WaveRoller array experiments is shown in Figure 2.

In the WaveDyn models, the PTO control function is implemented through a lookup table that relates the PTO velocity to the applied force. For each simulation, a linearised damping profile was estimated from the tank measurements. A realistic model that includes in addition a residual coulomb friction force and stiffness was considered. The estimation of the damping was made through a multivariable least square fit function of the tank measurements to the model:

$$F_{PTO} = F_{fric} + k_{stiff}\, x_{PTO} + k_{damp}\, v_{PTO}$$

where F_{fric} is the coloumb friction force, k_{stiff} and k_{damp} are the stiffness and damping coefficients and x_{PTO} and v_{PTO} the displacement and velocity of the PTO joint.

An example of the relationship between the angular velocity and moment in the PTO that was used to estimate the damping and stiffness coefficient for the WaveDyn simulations is shown in Figure 8 by the blue line. In the same plot, the red line corresponds to the WaveDyn simulation results. It is clear that for this particular test, the controller could not keep a perfect linear relationship at all times. The test was performed for an equivalent full scale regular wave of H=1.5m and T=9s, with a single WaveRoller.

For the same test, the time series associated with the measured PTO variables are shown in Figure 9 (blue line). The red line shows the outputs from the WaveDyn simulation. In the Figure, the top plot shows the surface elevation measured in absence of the models, followed by the angular position, velocity and moment. The last plot shows the time series for the instantaneous absorbed power. It is noted that large reflections in the tank mean that it is very unlikely that the measured excitation wave will be perfectly sinusoidal.

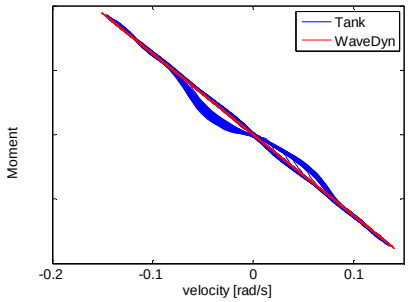

Figure 8: Relationship between the velocity and moment in the PTO for a test with a regular wave (H=1.5m T=9s)

To improve the WaveDyn comparisons with the measurements, the input wave in the simulation replicates the one measured during the calibration phase, at the location of the scale model (wave probe 9, see Figure 4). A trigger signal that could be used to synchronise the signals from different DAQs was unfortunately unavailable. As an alternative, the signals from the calibration waves and experiments were synchronised manually by overlapping the initial part of the signal from a common reference wave probe (number 1, Figure 4) located upstream and away from the scale models.

The comparisons of the time series signals in Figure 9 show that WaveDyn is able to reproduce quite closely the performance of WaveRoller in the experimental tests. The steady-state amplitudes of the signals are presented in Table 2, showing differences that are less than 1%.

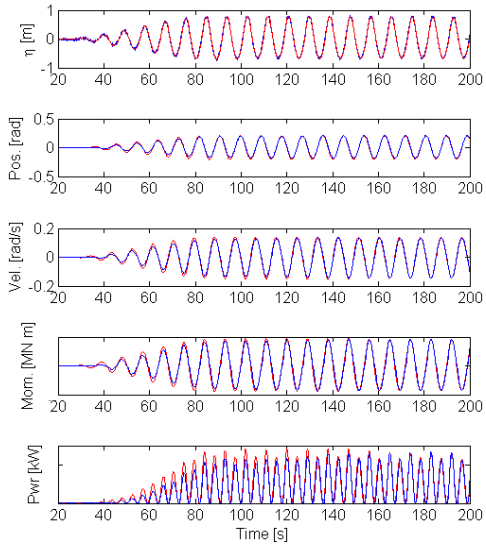

Figure 9: Comparison between the time series of measured variables (blue line) and WaveDyn simulations (red line) for a single flap in a regular wave (H=1.5m, T=9s)

The small deviations from the measurements are mostly due to the nonlinear characteristics in the PTO. It is noted that these results are still preliminary and agreement may be further improved by providing WaveDyn with a PTO relationship that more closely reproduces the one from the experiments. A non-linear excitation force implementation is also available in WaveDyn, which may be expected to further improve the numerical predictions.

Figure 10, shows the time series associated with the array experiments in unidirectional irregular waves for two of the WaveRollers scale models. The results indicate that WaveDyn is able to reproduce closely the model response measured during the experiments. Most of the observed differences are attributed to the non-linear characteristics of the scale model PTO and to the differences in the wave kinematics (although the measured surface elevation was input into WaveDyn, the effect of reflections was not fully accounted for).

During the experiments, the waves radiated and reflected from the models are reflected back from the

wave paddles, causing a further interference with the incident wave which cannot be accounted for in the wave calibration data set. This effect might be reduced with the use of wave paddles with active absorption but is very difficult to account for in a numerical model.

Table 2: Amplitude for the time series signals shown in Figure 9

	Pos. (rad)	Vel. (rad/s)	Mom. (%Err)
Tank	0.197	0.138	-
WaveDyn	0.199	0.139	0.69 %

6. Conclusions

This paper describes the WaveDyn models that were built to reproduce the experimental tests undertaken by AW Energy at CEDEX wave basin. The tests were performed for a WaveRoller scale model in isolation and for an array composed of three machines sitting side-by-side.

The preliminary results show that WaveDyn, an independent, general purpose (not machine specific) multi-body WEC modelling code, is able to reproduce the measured PTO variables and provides a reliable estimation of the performance of the WaveRoller machine. The differences between the tank measurements and WaveDyn predictions are mainly caused by the differences in the measured and modelled PTO profiles and the differences in the wave kinematics due to reflected waves in the tank. Both these effects would be less important for a full scale device operating in open water. A more comprehensive set of comparisons will be completed once tank data for the remaining array configurations has been processed.

References

[1] WAMIT - User Manual (Versions 6.4). WAMIT, Inc., 2006. URL www.wamit.

[2] Cummins, W. E. The impulse response function and ship motions. Schiffstechnik, 1962, 47, pp:101-109

[3] J. Falnes. Ocean waves and oscillating systems. Cambridge University Press, 2002.

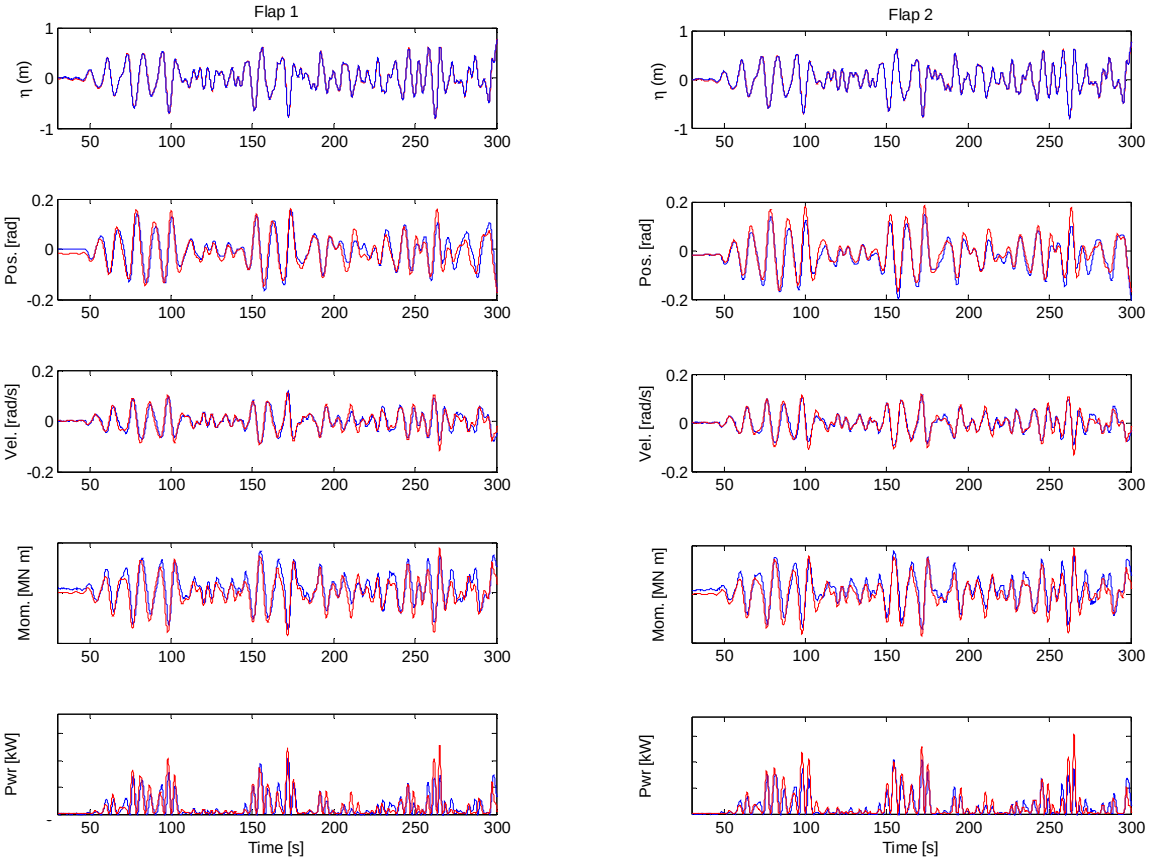

Figure 10: Comparison between the time series of measured variables (blue line) and WaveDyn simulations (red line) for an array in unidirectional irregular wave (Hm0=1.5, Te=10s)